

Electrical properties of vacuum evaporated PbSnS₃ thin films

T. A. KUKU, S. O. AZI, O. OSASONA

Department of Electronic and Electrical Engineering, Obafemi Awolowo University, Ile-Ife, Nigeria

Published online: 4 February 2006

Electrical conduction of evaporated PbSnS₃ films of thickness ranging between 0.1 and 2.0 μm were studied by measuring the dc current in both parallel (planar) and transverse (cross plane) directions to the substrate surface. Conduction mechanisms relevant to various regions of the current-voltage characteristics are discussed. The obtained film conductivities were of the order $10^{-5} \text{ S cm}^{-1}$ at room temperature and increased exponentially with increasing temperature. No consistent modification of the conductivity values and nature were observed when the films are doped with CdCl₂, PbCl₂ and CuI impurities. While planar conductivity activation energies were constant with voltage and increased slightly with deposition temperature, the cross plane values were found to depend on both voltage and film deposition temperature.

© 2006 Springer Science + Business Media, Inc.

1. Introduction

In line with the search for new ternary compounds for optoelectronic applications, single crystals of PbSnS₃ have been grown and their properties cursorily examined [1]. The crystals have an orthorhombic crystal symmetry and are characterized by SnS₆ octahedra chains parallel to the crystallographic *c*-axis. Optical band gap of these crystals is at 1.05 eV and electrical conductivity studies on them in the temperature range –100 to 500 K gave an activation energy, E_a , of 0.9 eV and room temperature conductivity of $10^{-6} \text{ S cm}^{-1}$. Also, the conductivity of this material decreased by three orders of magnitude under pressure of up to 120 k bar at room temperature [2].

Recently, thermally evaporated PbSnS₃ thin films (hereafter referred to as LTS) have been found to be very stable and their optical gap is 1.04 eV [3, 4]. The component elements of this compound are cheap and abundant. It could therefore become attractive for thin film photovoltaic applications.

The measurements of both planar and cross plane dc current in thermally evaporated LTS films, as a further attempt to unfold its electrical properties, is reported in this paper.

2. Experimental

LTS films were deposited on Corning 7059 glass substrates in the temperature range 300 to 500 K in an Edwards High Vacuum System pumped down to a pressure of about 10^{-3} Pa. Details of the evaporation technique,

source preparation composition and X-ray data of the films are as reported previously [3, 4]. The films used in this study ranged in thickness from 0.1 to 2.0 μm and were deposited at a rate of about 1.5 nms^{-1} . Some of the films were doped with CdCl₂, PbCl₂ and CuI achieved by a co-evaporation process.

For planar current flow, 1.0 cm \times 1.0 cm films were deposited on Corning 7059 glass substrates and two different contact configurations were employed. Firstly, Al contacts were deposited on opposite sides such that they overlap the film by 0.1 cm, thus defining an effective film dimension of 0.8 cm \times 1.0 cm. Secondly, four 0.1 cm² Al contacts were deposited at the corners of the film for Van der Pauw configuration. For cross plane current flow, the substrate was first coated with a bottom Al contact. Subsequent to LTS evaporation on the coated glass, top metal contacts (0.25 cm²) were deposited through a wire grid, thus forming either Al/LTS/Al, for symmetric or Al/LTS/Sn, for an asymmetric metal-semiconductor-metal (MSM) sandwich structure. Electrical leads were bound to the contacts with silver paste.

A Chromel Alumel thermocouple was mechanically attached to the substrate surface for the film temperature measurement. The film-substrate couple was then mounted firmly on a stainless steel heating pad. All measurements were carried out in an evacuated glass tube ($\sim 10^{-1}$ Pa). The tube was slipped into a metal sheath to avoid undesirable photoeffects and measurements were taken only when the current stabilised at a particular temperature. Voltages of 0.1 to 15 V were applied across the

films for planar and 0.005 to 1.0 V for cross plane current flow. The films were driven by a Phillips 6201B stabilised power supply, while the current was measured with a Leybold – Heraeus 53200 current amplifier.

3. Results and discussion

3.1. Planar current flow

The log-log plot of current-voltage characteristics of undoped LTS film deposited at room temperature is shown in Fig. 1. Through the range of applied voltages, the current increased from 10^{-11} to 10^{-9} A at 300 K, and from 10^{-9} to 10^{-7} A at 420 K. Doped films gave similar range of current. The current-voltage plot shows a linear relationship which extends well into higher voltages, (15 V) though not indicated in the figure. The characteristics of the films deposited at higher temperature is also linear, indicating that the same conduction process is probably at play. The slope of these curves is about 0.97, a number close to 1.0, which is characteristic of ohmic conduction. This is hardly surprising, since low electric fields, (about 10 V/cm) are applied across the films.

Arrhenius plots of conductivity for LTS films with different thickness, for both heating and cooling cycles, are presented in Fig. 2. During the heating cycle and below 340 K, the 0.120 μm film exhibited enhanced conductivities that were weakly dependent on temperature. This may be regarded as the extrinsic conduction, which is determined by a host of factors, including intercrystallite barrier, strain, absorbed gases, and non-stoichiometry [5, 6]. The intrinsic region, where conductivity rises exponentially with temperature, is clearly seen above 340 K. During the cooling cycles, all films gave lower conductivities which is well described by a temperature activated

process in which $\sigma = \sigma_0 \exp(-E_a/kT)$, where σ_0 is the preexponential factor and E_a the activation energy. Therefore the E_a obtained from the cooling curves is thought to be more representative of the conduction process in these films. Also, the reduced presence of extrinsic regions in the cooling cycles suggests that some of the associated defects or impurities have been neutralised and some of the absorbed gases desorbed from film surfaces by the heating/annealing stage. We in fact observe that there was no significant change in the conductivity trend for subsequent heating and cooling cycles. It is significant to note that the film conductivity obtained from Van der Pauw's method were not different from that calculated from simple current-voltage measurements.

The conductivity and activation energy of both undoped and doped LTS films deposited at various temperatures are presented in Table I. The table shows the same conductivity range for both classes of films deposited in the temperature range of 300 to 473 K. Doping seems not to have affected the conductivity of the films in any consistent manner since no consistent increase or decrease in conductivity or activation energy is observed, except for thicker films when slightly increased conductivity and a slight change in activation energy from about 0.7 to 0.6 eV were observed. In all cases, the level of doping was estimated to be about 5 mol% of film composition. The undoped material is *p*-type conducting. The idea was to see if doping with halides having excess electrons will affect the conductivity. The fact that there is no consistent behaviour of dopants on this material may indicate that it might be difficult to dope. Supposedly in a ternary material like LTS, non metal substitutional atoms in Pb and Sn sites should act as donors and metal substitutional atom on S sites as acceptors. Thus charged native defects

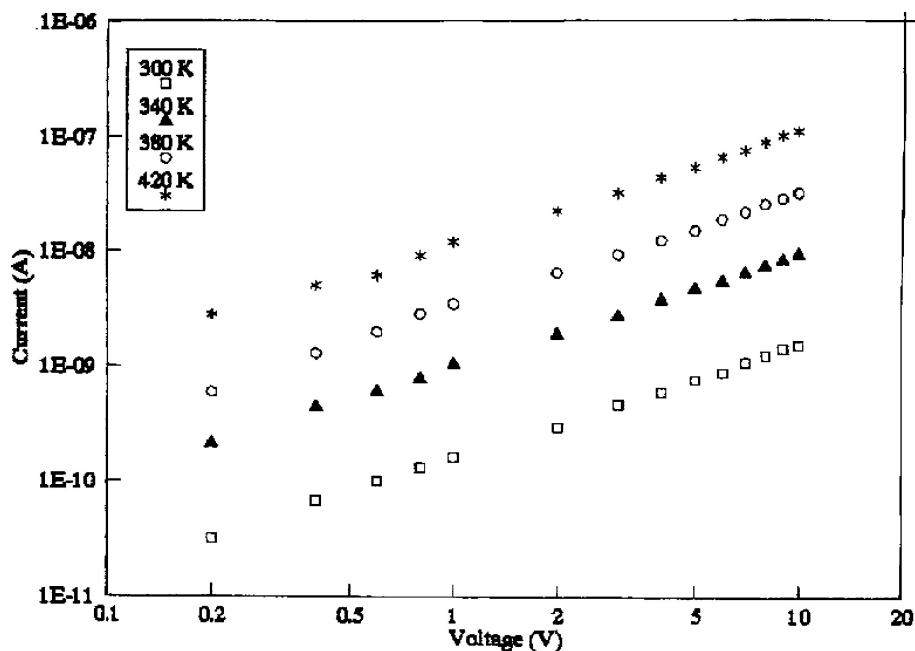


Figure 1 In-plane current-voltage characteristics of evaporated PbSnS_3 thin films.

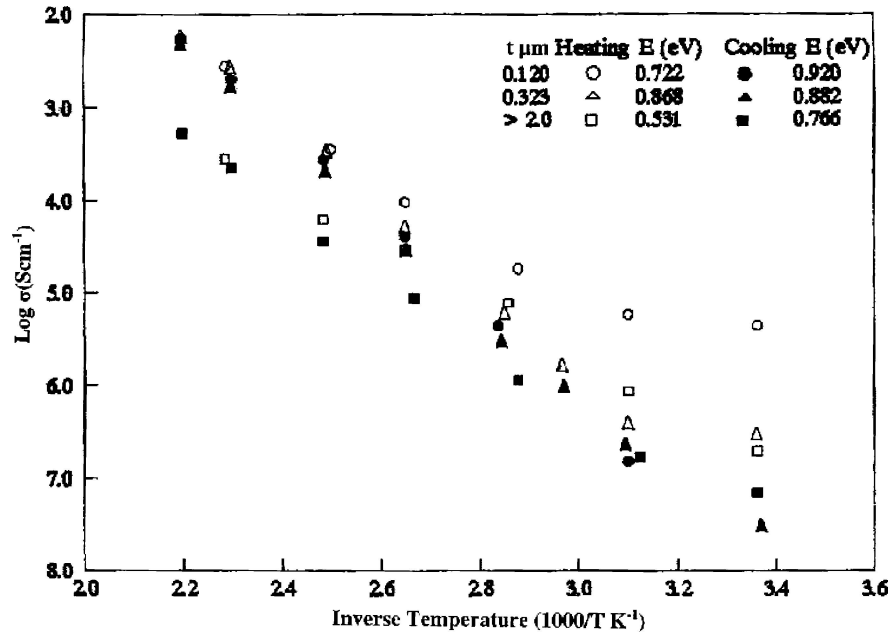


Figure 2 Temperature dependence of the conductivity of PbSnS₃ thin films with thickness as a parameter.

arising either from Pb⁺ and Sn⁺ cations on S sites or S⁻ anions on the metal sites dominate the electrical properties [7]. This probably explains why ternary compounds such as CuInSe₂, CuGaSe₂ and ZnGeP₂, to mention a few, are difficult to dope [8–10].

E_a and conductivity for films deposited at 340 K is apparently higher. It has been reported [11] that materials tend to have a deposition temperature at which all film properties are optimised. Such a process could be responsible for this observation. Otherwise, E_a tends to decrease with deposition temperature. This trend is probably due to the increased crystallinity with increasing deposition temperature, as can be seen in Table I.

3.2. Cross plane current flow

The current voltage (I-V) curves of an Al/LTS/Al sandwich structure are presented in Fig. 3. The film conduction process changes rather sharply from ohmic into trap law conduction regions, as can be seen in the abrupt transition of the I-V curves. The transition becomes less abrupt as film temperature increases. This phenomenon is not unrelated to thermal detrapping of charge carriers

at elevated temperatures [11]. The Al⁺/LTS/Sn (positive potential applied to the Al contact) structure showed similar features. In the case of Al/LTS/Al, the structure could not be driven beyond 1.0 V, which corresponds to an electric field of about 10⁵ V/cm across the film.

In general, thin film I-V curves can be modelled by [12]

$$I \propto V^m \quad (1)$$

where m is known as the non-linearity coefficient and has a value of $m = 1$ for the low field ohmic conduction region. Beyond this region, $m \geq 1$, which is often referred to as the varistor regime [13, 14]. The values of m obtained for the curves in Fig. 3 in the regime at 300, 360, and 385 K were 36, 12, and 6.8, respectively, indicating that the carrier generation process is mostly controlled by thermionic emission across grain barriers [15]. At about 1.0 V, the corresponding electric field across a typical film of about 0.5 μm thick is of the order of 10⁴ V/cm. This is the threshold field for dielectric breakdown [12]. Indeed, some of the Al/LTS/Al structures driven just beyond 1.0 V were permanently destroyed. Thus the rapid

TABLE I. The dependence of conductivity on deposition temperature, and hence crystallite size, for undoped and doped films of PbSnS₃. The activation energy, E_a is for the conductivity measurement in the temperature range 300 to 450 K, and for the range of conductivity values indicated

| Crystallite size (μm) | σ range (S cm ⁻¹) × 10 ⁻³ for temp. 300–450 K | Deposition temperature (K) | E_a (eV) | | | |
|-----------------------|---|----------------------------|------------|-------------------|-------------------|-------|
| | | | Undoped | Doped | | |
| | | | | CdCl ₂ | PbCl ₂ | CuI |
| <0.15 | 0.05–2.0 | 300 | 0.83 | 0.793 | 0.835 | 0.793 |
| 0.35 | 0.02–5.0 | 340 | 0.85 | 0.835 | 0.862 | 0.794 |
| 0.38 | 0.001–1.0 | 400 | 0.76 | 0.880 | 0.792 | 0.776 |
| 0.5 | 0.005–1.0 | 473 | 0.72 | 0.610 | 0.603 | 0.600 |

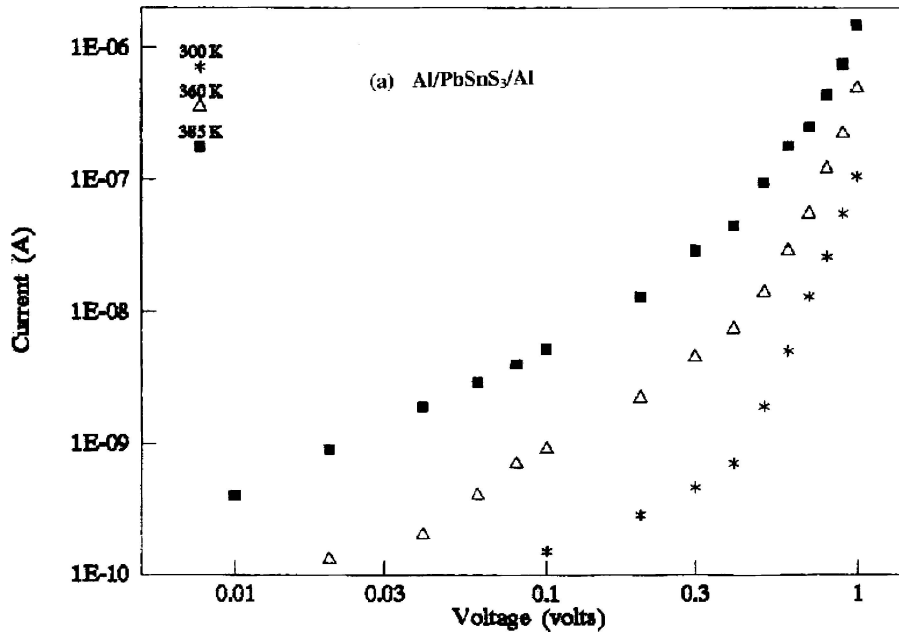


Figure 3 Current-Voltage characteristic of Al/PbSnS₃/Al capacitor structure at different temperatures.

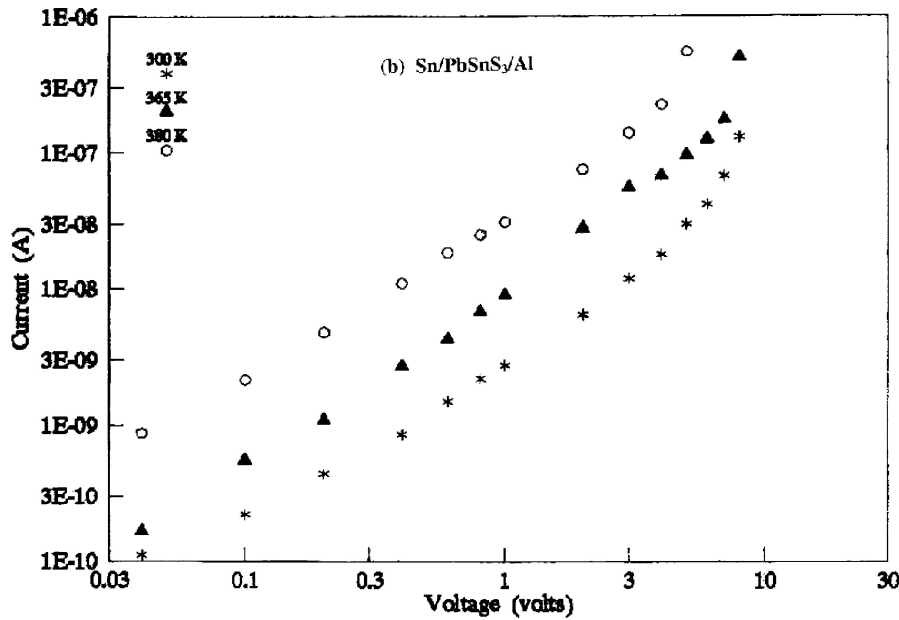


Figure 4 Current-voltage characteristics of Sn/PbSnS₃/Al capacitor structure at different temperatures.

current increase when LTS MSM sandwich structures are subjected to this field intensity truly indicates the onset of electrical breakdown.

The barrier height of MSM structures, ϕ_b , can be calculated from current density (J) versus voltage (V) curve, since in general the J-V relationship is of the form [12]

$$J = J_s(e^{qV/kT} - 1) \quad (2)$$

with

$$J_s = A^{**}T^2 \exp(-q\phi_b/kT) \quad (3)$$

where A^{**} is the effective Richardson constant, T is absolute temperature while other components have their usual meanings. The extrapolated value of current density at zero voltage is the saturation current, J_s , and the barrier height can be obtained from the equation

$$\phi_b = (kT/q) \ln(A^{**}T^2/J_s) \quad (4)$$

For the I-V curves of Fig. 3, J-V plots were determined by the use of the effective contact area of the upper electrode of the MSM sandwich structure ($A = 0.25 \text{ cm}^2$). Fitting the extrapolated values of J_s at $V = 0$ to Equation (4) gave the values of the barrier height at the different

TABLE II. Barrier heights obtained for different applied voltages for measurements in the temperature range 300 to 390 K for the symmetric MSM sandwich structure

| Voltages (V) | E_a (eV) ($300 \leq T \leq 390$ K) |
|--------------|---------------------------------------|
| 0.1 | 0.860 |
| 0.4 | 0.842 |
| 0.6 | 0.786 |
| 0.8 | 0.702 |
| 1.0 | 0.606 |

temperatures to be 0.875 eV (300 K), 0.853 eV (360 K) and 0.837 eV (385 K). There appears to be a general decrease with increasing temperature.

Apart from determining the contact potential value from the J-V curve, it has been established that an activation energy plot gives a better and more accurate value of ϕ_b [12]. In this case, the current curves are extrapolated to zero voltage to give I_o for each temperature. A plot of $\ln I_o$ versus $1/T$ should give the zero voltage barrier height, ϕ_{bo} . The slope of this plot may be written as [11]

$$E_a = k\partial(\ln I_o)/\partial(1/T) \quad (5)$$

and

$$I_o = A'/\exp\{-\phi_{bo}/kT\} \quad (6)$$

giving E_a as

$$E_a \approx \phi_{bo} - T\partial\phi_{bo}/\partial T \quad (7)$$

if the barrier height is temperature or voltage dependent. Thus, the Arrhenius plot of I_o does not in general give ϕ_{bo} . This is equally true of such plots at non zero voltages and in particular, ϕ_b collapses in the varistor region. Barrier heights calculated from Arrhenius plots of the I-V data of Fig. 3 at various voltages are presented in Table II. The general decrease with increasing voltage is clearly seen in the table.

Suprisingly, Al/LTS/Sn⁺ structures could be driven up to 7.8 V as seen in Fig. 4. It is apparent that the conduction mechanisms outlined above are not exhibited by these curves. Again, the more gradual transition of the curves at higher temperatures is seen in the figure at about 7.0 V. Further work is in progress to clarify the apparent rectifying nature of the Sn/LTS contact.

4. Conclusion

The evaporated LTS thin films exhibit ohmic conduction at low fields ($\leq 10^4$ Vcm⁻¹) and non ohmic conduction at higher fields. Activation energies obtained from planar current flow range between 0.72 and 0.85 eV (and are not affected in any consistent manner by doping with halide impurities), as film deposition temperature decreased from 473 to 300 K. Those obtained from transverse current flow are dependent on voltage and temperature. Current-voltage curves of the evaporated MSM structures clearly exhibit ohmic conduction at low electric fields and highly non-ohmic behaviour beyond the threshold for dielectric breakdown. The films also show asymmetric electrical behaviour when sandwiched between Al and Sn electrodes.

Acknowledgements

Financial support from TWAS, As-ICTP and SIDA, Italy, is gratefully acknowledged.

References

1. V. U. ALPEN, J. FENNER and E. GMELIN, *Mater. Res. Bull.* **10** (1975) 175.
2. H. R. CHANDRASEKHAR and D. G. MEAD, *Phys. Rev. B*: **19** (1979) 932.
3. T. A. KUKU and S. O. AZI, in "Renewable Energy Technology and the Environment," edited by A. A. M. Sayigh (Pergamon, Oxford, 1992) Vol. 1, p. 297.
4. *Idem.*, *J. Mater. Sci.* **33** (1998) 3193.
5. O. S. HEAVENS, "Thin Film Physics" (Methuen, London, 1970) p. 7.
6. J. P. ENRIQUEZ and S. MATHEW, *Solar Energy Mater. Solar Cells* **76** (2003) 313.
7. J. A. GROENINK and P. H. JASSE, *Zeitschrift fur Physikalische Chemie Neue Folge* **110** (1978) 17.
8. N. B. HANNAY and U. COLOMBO, "Electronic Materials" (Academic Press, New York, 1973) p. 479.
9. A. MEEDER, L. WEINHARDT, R. STRESING, D. FUERTES MARRON R. WURZ, S. M. BABU, T. SCHEDEL-NIEDRIG, M. C. L. STEINER, C. HESKE and E. UMBACH, *J. Phys. Chem. Solids* **64** (2003) 1553.
10. G. A. MEDVEDKIN, P. G. BARANOV and S. I. GOLOSHCHAPOV, *ibid.* **64** (2003) 1691.
11. G. E. PIKE and C. H. SEAGER, *J. Appl. Phys.* **50** (1979) 3414.
12. S. M. SZE, "Physics of Semiconductor Devices" (John Wiley, New York, 1981) p. 5.
13. R. D. GOULD, *Thin Solid Films* **125** (1985) 63.
14. J.-H. TAN and W. A. ANDERSON, *Solar Energy Mater & Solar Cells* **77** (2003) 283.
15. S. ASHOK and K. P. PANDE, *Solar Cells* **14** (1985) 61.

Received 24 November 2003

and accepted 9 May 2005